

# URGENT SCIENTIFIC AND TECHNICAL CHALLENGES AT INCREASE OF ENERGY EFFICIENCY OF ALUMINIUM REDUCTION CELLS

*Ye.N. Panov, A.Ya. Karvatsky, I.L. Shilovich, G.N. Vasilchenko, T.B. Shilovich,  
S.V. Leleka, S.V. Danilenko, V.V. Bilko, I.V. Pulinets, A.N. Chizh*

National Technical University of Ukraine «Kiev Polytechnic Institute», Kiev, Ukraine

## Introduction

Increase of energy cost is highly significant for energy-intensive industrial branches, in particular, for competitiveness of aluminium producers. Therefore, the development and construction of electrolysis cells with decreased specific power consumption and increased lifetime of cathode assembly are of vital importance.

Nowadays numerous projects are under intensive development devoted to the electrolysis cells of this type with consideration of preliminary MHD estimations, power and mechanical properties supported with subsequent engineering projects. However, rather frequently the anticipated results do not match actual consequences. One of the major reasons is a set of uncertainties at every stage of development. This is relevant both for methods of modeling of electrolysis cell state, and for influence of changes in technological schedule and properties of involved raw materials on technological process, and for changes of properties of raw materials depending on supplier and manufacturing process, external factors and so on.

This report discusses only some of the challenges we met at solution of actual problems, however, we believe, that the discussed scope of the challenges prevents the achievement of reliable approaches and requires for conductance of supplemental investigations.

It should be noted, that the development of «successful» design of electrolysis cell results in significantly higher cost savings than the investments into the conductance of such supplemental investigations.

## Effect of physical fields of electrolysis cell on its power state

An aluminium electrolysis cell (Figure 1) is a high-temperature energy-intensive industrial assembly operating with chemically aggressive substances (molten electrolyte and meta), the thermal strains of its structures reach maximal allowable values of refractoriness and strength recommended for the structural materials. Therefore, the requirements to the design, selection of structural materials and electrolysis technology applied at aluminium electrolysis cell are the determining factors effecting on the electrolysis cell efficiency and lifetime.

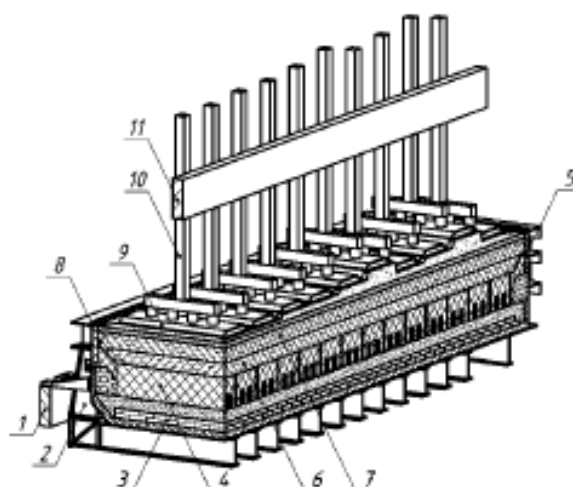


Fig. 1. 320 kA PB cell

- 1 – cathode busbar; 2 – cradle cathode shell; 3 – foundation refractory lining;  
4 – bottom section; 5 – side wall block; 6 – metal; 7 – electrolyte; 8 – sludge and ledge;  
9 – prebaked anode; 10 – anode bar; 11 – anode busbar

The major parameters determining the energy efficiency of electrolysis cell operation are current efficiency and specific power consumption. Their energy balance was and remains a powerful tool of estimation of electrolysis cell power state. Therefore, the development of new electrolysis cells and retrofitting of existing ones are based on wide application of energy balance of electrolysis cells, allowing to estimate both overall energy efficiency of electrolysis cells, and its individual components, as well as to determine possible reserves and the ways to decrease specific power consumption and to increase current efficiency. In other words, it can be stated that the theoretical balance is an energy ID of electrolysis cell. However, at increase of operation time of electrolysis cell its energy efficiency decreases, mainly due to increase of heat losses from cathode basement area as a result of lining saturation with molten electrolyte and metal together with some other factors.

«Power-Saving Technologies» R&D Center at «Kyiv Polytechnic Institute» gained wide experience in the field of calculation and estimation of energy balances for electrolysis cells of various types and designs (Figure 2) by means of computational empiric methods, modern tools of field experiments and numerical simulation of physical fields [1 – 4].

Numerical simulation of physical processes in aluminium electrolysis cells considers the following interrelated and independent problems of mathematical physics with accounting for contact interactions between interconnected structural elements of various physical essence, namely: thermal-electrical – Figure 3(a, b), mechanical – (Figure 3(c)) and magneto-hydrodynamic [5].

In practice, the most important operational parameters required for the electrolysis process can be sufficiently determined by solution of thermal-electrical problem with the use of efficient heat-transfer coefficients considering for flows of molten electrolyte and metal [4], the obtained solution is subsequently used for calculation of energy balance of aluminium electrolysis cell.

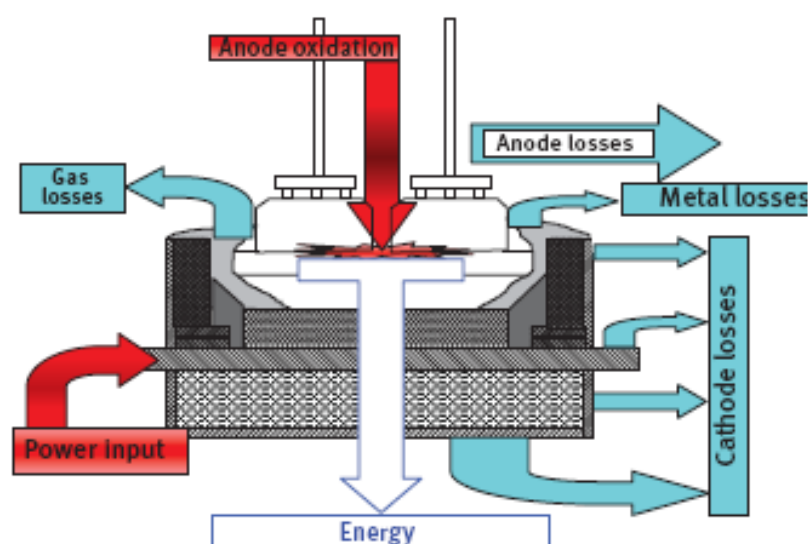


Fig. 2. Schematic diagram of energy balance in terms of ambient temperature

Currently, solution of the dynamic problems is of growing interest, their solution allows to trace virtually the transient processes in aluminium electrolysis cells at the design stage, namely: start-up states, metal pad perturbations and distortions, anode effects, anode replacement, electric power modifications and so on.

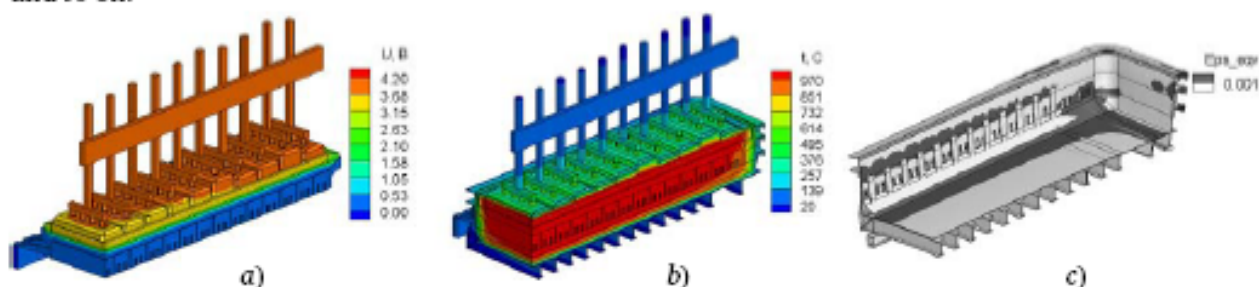


Fig. 3. Thermo-electro-mechanical state of high-amperage (320 kA) aluminium PB cell at operation a, b) electric and temperature potential fields; c) Mises equivalent cathode plastic deformation (the areas of residual strains are marked with black color)

Non-stationary (dynamic) thermo-electric state of an aluminium electrolysis cell (Figure 1) with consideration of magneto-hydrodynamics of molten electrolyte and metal, moving phase interface between the molten substances and sludge and ledge, in general case can be described by Navier-Stokes equation set accounting for turbulence in the  $k - \varepsilon$  model approximation and Maxwell equation set that includes the equations of energy, motion conservation, continuity, electric potential, magnetic field eddy, electric current density and magnetic induction:

$$\left\{ \begin{array}{l} c_p(t)\rho(t)\frac{\partial t}{\partial \tau} + c_p(t)\rho(t)\nabla \cdot (\mathbf{V}t(X)) = \nabla \cdot \left[ \left[ \lambda(t) + c_p(t)\eta_t \right] \nabla t(X) \right] + \frac{\mathbf{j} \cdot \mathbf{j}}{\chi(t)} + \eta\Phi, \\ \frac{\partial(\rho(t)\mathbf{V})}{\partial \tau} + (\rho(t)\mathbf{V} \cdot \nabla)\mathbf{V} = -\rho(t)\mathbf{g} - \nabla p + \nabla \cdot \left\{ \eta(t) \left[ (\nabla\mathbf{V} + \nabla\mathbf{V}^T) - \frac{2}{3}\nabla\mathbf{V}\delta_{ij} \right] \right\} + \mathbf{j} \times \mathbf{B}, \quad i, j = \overline{1,3}, \\ \frac{\partial\rho(t)}{\partial \tau} + \nabla \cdot (\rho(t)\mathbf{V}) = 0, \\ \rho(t)\frac{\partial k}{\partial \tau} + \nabla \cdot (\rho(t)\mathbf{V}k) = \nabla \cdot \left( \left( \eta(t) + \frac{\eta_t}{\sigma_k} \right) \nabla k \right) + G - \rho(t)\varepsilon, \\ \rho(t)\frac{\partial \varepsilon}{\partial \tau} + \nabla \cdot (\rho(t)\mathbf{V}\varepsilon) = \nabla \cdot \left( \left( \eta(t) + \frac{\eta_t}{\sigma_\varepsilon} \right) \nabla \varepsilon \right) + \frac{\varepsilon}{k} (C_1 G - C_2 \rho(t)\varepsilon), \\ \nabla \mathbf{j} = 0, \\ \nabla \times \mathbf{H} = \mathbf{j}, \\ \mathbf{j} = -\chi(t)(\nabla U - \mathbf{V} \times \mathbf{B}), \\ \mathbf{B} = \mu\mu_0 \mathbf{H}, \end{array} \right. \quad (1)$$

where  $c_p$  – specific isobar thermal capacity, J/(kg·K);  $\rho$  – density, kg/m<sup>3</sup>;  $\tau$  – time, s;  $\mathbf{V}^T = (V_x, V_y, V_z)$  – velocity vector, m/s;  $\nabla = \left( \frac{\partial}{\partial x}, \frac{\partial}{\partial y}, \frac{\partial}{\partial z} \right)$  – Hamiltonian operator;  $t$  – temperature, °C;  $\lambda$  – heat conductivity, W/(m·K);  $X(x, y, z) \in R^3$  – Cartesian ordinates, m;  $\eta_t = C_\eta \rho \frac{k^2}{\varepsilon}$  – turbulent viscosity coefficient, Pa·s;  $k$  – turbulent energy, m<sup>2</sup>/s<sup>2</sup>;  $\varepsilon$  – turbulent energy dissipation rate, m<sup>2</sup>/s<sup>3</sup>;  $\sigma_k, \sigma_\varepsilon, C_\eta, C_1, C_2$  – parameters (constants) of standard  $k - \varepsilon$  model;  $G = \eta_t \frac{\partial V_i}{\partial x_j} \left( \frac{\partial V_i}{\partial x_j} + \frac{\partial V_j}{\partial x_i} \right), i, j = \overline{1,3}$ ;  $\mathbf{j}$  – electric current density vector, A/m<sup>2</sup>;  $\chi$  – electric conductivity, (Ohm·m)<sup>-1</sup>;  $\eta$  – dynamic viscosity, Pa·s;  $\Phi$  – energy dissipation, 1/s<sup>2</sup>;  $\mathbf{g}$  – gravity acceleration vector, m/s<sup>2</sup>;  $p$  – pressure, Pa;  $\delta_{ij}$  – Kronecker symbol;  $\mathbf{B}$  – magnetic field inductance vector, T;  $\mathbf{H}$  – magnetic field intensity, A/m;  $U$  – electric potential, V;  $\mu_0$  – magnetic constant, H/m;  $\mu$  – media relative magnetic permeability.

With the aim of unambiguity (1) the appropriate initial and boundary terms are defined, including the Stefan term at moving melt-sludge interface and ledge in explicit form (2); the Marangoni term at melt-gas free interface under anode assembly and crust, between the electrolyte and metal melts (3).

The Stefan terms at moving interfaces between electrolyte-sludge and metal-ledge are as follows

$$\left\{ \begin{array}{l} t|_s = t|_l \\ \{\mathbf{n} \cdot \mathbf{q}_k\} = \rho_s L_f \frac{\partial \mathbf{n}}{\partial \tau}, \end{array} \right. \quad (2)$$

where  $L$  and  $g$  – relate to liquid and gas, respectively;

$\{\mathbf{n} \cdot \mathbf{q}_k\} = \mathbf{n} \cdot \mathbf{q}_k^+ - \mathbf{n} \cdot \mathbf{q}_k^-$ ;  $\mathbf{n}$  – normal to phase interface surface;

$\mathbf{q}_k$  – heat flux density at moving interface;

$L_f$  – phase transition specific heat, J/kg;

$\rho_s$  – density of solid sludge buildup, kg/m<sup>3</sup>.

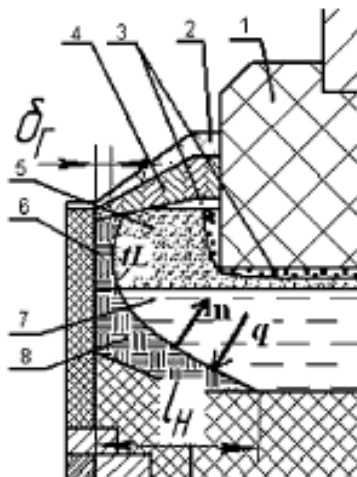


Fig. 4. Schematic presentation of cell smelting geometry and gas cavities, illustrating the setting of the Stefan and Marangoni boundary terms. 1 – Prebaked anode; 2 – alumina cover; 3 – gas cavities; 4 – crust; 5 – electrolyte; 6 – sludge; 7 – metal; 8 – ledge



At free liquid-gas interfaces (thermal capillary convection – the Marangoni terms) we have:

$$\begin{cases} \mathbf{n} \cdot \boldsymbol{\tau}|_L = \mathbf{n} \cdot \boldsymbol{\tau}|_g + \frac{d\sigma_{ST}}{dT} \nabla T \\ \boldsymbol{\tau} = \eta(\nabla \mathbf{V} + \nabla \mathbf{V}^T) \end{cases}, \quad (3)$$

where  $\sigma_{ST}$  – surface tension force, N/m;  $\boldsymbol{\tau}$  – stress tensor, Pa.

Similar terms (3) are considered at the free interface between metal and electrolyte melts.

Numerical solution of the non-linear system of equations (1)–(3) is sufficiently complicated task. The problem of the (1) type in 2D and 3D variants can be solved by various numerical methods beginning from the finite difference method and to the finite element method and finite volume method. This is supported both with proprietary software and commercial packages, such as ANSYS, CFX, Fluent, STAR-CD and so on.

The most efficient numerical method of solution of CFD-problems (computer fluid dynamic) is the finite volume method; its obvious advantage in comparison with other numerical methods is that it follows the fundamental law of energy preservation in each computational mesh independently on the discretization parameters of computational area, that is, it does not depend on the dimensions and number of computational meshes. Therefore, the finite volume method provides capability to create conservative discrete analogs of initial differential equations at the stage of its formulation, because the starting point of the finite volume method is the integral formulation of the laws of conservation of mass, momentum, energy etc. (Gauss formula for divergence and Gauss-Ostrogradsky theorem). The integral correlations of the finite volume method are written for random reference volume and their discrete analog is determined by summation over all edges of finite flows of momentums, mass etc. on the basis of respective quadrature formulas. And as the integral formulation of the conservation laws does not impose limitation on the shape of reference volume, the finite volume method can be applied for discretization of the fluid dynamics equations both on structured and non-structured grids with various mesh geometry, thus, none limitations are imposed on the degree of complexity of computational area geometry. Moreover, the finite volume method can be advantageously applied both for the problems of fluid dynamics, and for the problems of thermal and electric conductance of solids, as well as for numerous problems of other kind, that is, for solution of interrelated problems.

«Power-Saving Technologies» R&D Center at «Kyiv Polytechnic Institute» gained wide experience in the field of solution of various problems of fluid dynamics related with the designing and engineering of sophisticated heat-exchange equipment. The finite volume method was used as a basis for development of appropriate software utilizing SIMPLE algorithm (Semi-Implicit Method for Pressure Linked Equations) [6] on non-staggered and staggered non-structured tetroidal and hexahedronoidal grids and based on parallel computing in OMP and MPI standards.

The developed software is adapted for multiprocessor PC (2, 4 processors), OS MS Windows XP and in addition can be also utilized at the cluster of HPC (High Performance Computing) Centre, NTUU «KPI»: 1 – 312 processor system, 44×4 Intel Xeon E5440 @ 2.83 GHz and 68×2 Intel Xeon 5160 @ 3.00 GHz, peak performance – 7 TFlops, OS: CentOS release 5.2. The developed software can also be adapted for solution of the given problem (1–3). In this variant the moving solid-liquid interface (cell smelting geometry) and free gas-liquid interface can be determined on the basis of dynamic grids in the regions with melts and anode gases.

**Energetics of anode process.** Anode process is in fact the major process of electrolysis. This is the place where aluminium reduction occurs. However, at designing and engineering stage the most intensive attention is paid to cathode assembly due to its determining significance for electrolysis cell operation life.

At estimation of the anode process major attention is traditionally paid to electric parameters: alumina decomposition voltage, counter EMF, voltage drop etc. However, it should be noted, that the reaction of anode carbon oxidation is exothermic, and its thermal effect amounts to 394 kJ/mol (at CO<sub>2</sub> formation). It is a well-known fact [7], that the thermal effect of CO and CO<sub>2</sub> formation is equivalent to anode over-voltage, that is, 1.167 V and 1.034 V, respectively. Estimation of the thermal power, released at anode carbon oxidation, demonstrates that it can achieve (in equivalent terms) at least 40% (depending on anode gas composition) of theoretical value of decomposition voltage. Changes in the mentioned thermal power value of the oxidation indicates the necessity to change the anode voltage.

A physical consequence of the heat release at anode is its transfer to anode body. For self-baking anodes the aforementioned heat is partially consumed by the process of coke formation. For prebaked anodes the utilization of the heat of oxygen chemisorption is useless, therefore, the heat is released to environment.

Coked carbon materials, serving as anode support, are in crystalline state under operating conditions and exist in the form of hexagonal lattice with carbon atoms in the lattice sites. It is a well-known fact that the anode coke is characterized with varying chemical activity determined by the lattice imperfections. On the other hand, it has been theoretically established, that at thermal processing of carbon materials the lattice imperfections are eliminated and the carbon structure is improved. Therefore, the oxygen chemisorption accompanied with the thermal effect occurs at the anode sections with the highest chemical activity, this property in its turn is the higher with the less ordered structure; thus, in the less active sections the physical adsorption takes place. Under such conditions the carbon-oxygen compounds have no definite composition. The anode process is a time-distributed chemical transformation of  $C_xO_y$  compounds into stable CO and  $CO_2$  compounds.

In addition, it should be noted, that the oxygen chemisorption process at carbon materials are accompanied with thermal effect releasing up to 420 kJ/mol. The mentioned heat is transferred directly to carbon anode promoting coking process of the binder. For self-baking anode the coking processes are not studied in terms of formation of carbon structure capable to active interaction with oxygen in the electrolysis process.

Therefore, it can be concluded that the application of prebaked or self-baking anodes is characterized with certain peculiarities and should be numerically estimated, that is, with which carbon materials (both pitches and cokes) the carbon oxidation will be more or less active.

**Two-phase media behavior.** At present there are no available methods for simulation of the process of desorption of carbon oxides from the anode surface. It is known, that at passivation of anode surface (decrease of chemical activity of carbon oxidation) the electric potential is increased up to the level sufficient for formation of carbon fluorides with subsequent drastic evolution of anode effects. At present great attention is paid to the simulation of gas bubble motion in electrolysis cells [8, 9]. Well-established phenomenological dependencies of two-phase flow hydrodynamics should be mentioned [10, 11]. The steady state of gas-liquid layer are estimated on the basis of well-known criteria:

– linear scale of capillary-gravitational interaction characterizing the dimensions of generated gas phase,  $\delta_{\sigma g} = \left( \frac{\sigma}{g\Delta\rho} \right)^{0.5}$ , where  $\sigma$  – surface tension, N/m;  $\Delta\rho = \rho' - \rho''$ ,  $\rho'$  – liquid density, kg/m<sup>3</sup>  $\rho''$  – gas density, kg/m<sup>3</sup>;

– criterion of gravitational-capillary-viscous interaction (modified Archimedes number)  $Ar = \frac{g\overline{\Delta\rho} \cdot R^3}{\nu'^2}$  where  $\overline{\Delta\rho} = \frac{\Delta\rho}{\rho'}$  – relative density;  $R$  – equivalent linear dimensions of a bubble, gaseous layer, m;  $\nu'$  – kinematic viscosity, m<sup>2</sup>/s.

The relative motion velocity of light phase is determined as follows:

$$U^* = CAr^n \frac{1 + \bar{\mu}}{a + b\bar{\mu}},$$

where  $\bar{\mu} = \frac{\mu''}{\mu'}$  – relative viscosity;  $\mu''$ ,  $\mu'$  – dynamic viscosity of gas and liquid, respectively, Pa · s.

In addition, it should be noted, that the gas-liquid systems agitated from under horizontal plane (as at bubble evacuation from anode) remain actually not investigated at present.

**Anode coking.** Presently the process of anode coking is not sufficiently investigated for operating electrolysis cells. The anode paste production technology is described in details elsewhere [14]. The anode coking schedule, being non-stationary thermal process, is determined by the electrolysis technological process. On the other hand, the theory and practice of carbon electrode production by means of baking and graphitization provide evidences that the baking schedules are sufficiently complicated thermal processes performed in accordance with sophisticated temperature profile; when this profile is maintained the prescheduled formation of coke mesophase occurs as well as gas evolution at pitch pyrolysis and coke formation.

The estimation of available experimental data evidences that at present the processes of gas formation at anode coking, the dependencies of formation of mesophase and final structures of carbon materials are not investigated in complete details. There is a lack of data on migration of gas and binder in anode, therefore, the properties of carbon structure on anode bottom and its reactivity cannot be determined.

Complex investigations of anode paste coking should be carried out, including experiments (measurements of anode temperature, gas evolution temperature range, composition and consumption of volatile matters etc.), as well as calculations (estimations of coking cone, association of the thermal parameters with anode dimensions and coke formation processes, etc.)



### Influence of impregnation of lining and thermal insulating materials on electrolysis properties and electrolysis cell lifetime

One of the most challenging parts of an electrolysis cells is the cathode assembly, consisting of metal shell, carbon cathode with current conductors, refractory lining and thermal insulation. It can be attributed to the fact that nearly all elements of cathode assembly are not replaceable and cannot be repaired on regular basis. On the other hand, the cathode assembly is a multi-purpose unit: provision of not only mechanical strength of the structure, but also of high power and technological performances of aluminium production. The latter are determined by the properties of carbon containing lining and refractory materials, as well as of thermal insulation.

*Overall problem of improvement of energy efficiency of aluminium production and increase of cathode lifetime can be solved only by means of integrated approach with consideration of the production technology, the schedule of preparation of an electrolysis cell for operation, properties of the involved materials, etc..*

One of the reasons resulting in deteriorating of an electrolysis cell operating performances and uncertain pattern of the thermal properties of cathode assembly is the changes of the properties of lining materials and thermal insulation during the overall life cycle of the electrolysis cell, starting from preheating stages and ending with the electrolysis cell shut-down. At initial stages the uncertain thermal properties of the cathode assembly depend mainly on the moisture content in the foundation.

Figure 1 illustrates the estimated regions of condensed moisture, water-steam mixture and overheated steam obtained on the basis of experimental data on temperatures in the electrolysis cell foundation in central half cross-section of an electrolysis cell. In the overheated steam region the moisture content decreases constantly with time, it can be considered as «dry region». The thermal conductance of the materials in this region corresponds to specifications of the initial material (confirmed with the results of laboratory analyses of dried materials). Expansion of this region into the insulating layers results in an increase of thermal resistivity of the discussed region and modifies the pattern of temperature distribution in the foundation. As a consequence, minimal amount of isotherms in the foundation bottom portion are moved to the periphery.

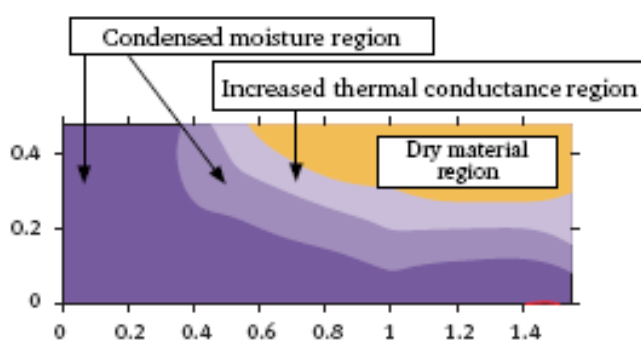


Fig. 5. Schematic presentation of moisture distribution in electrolysis cell foundation after 14-hour baking

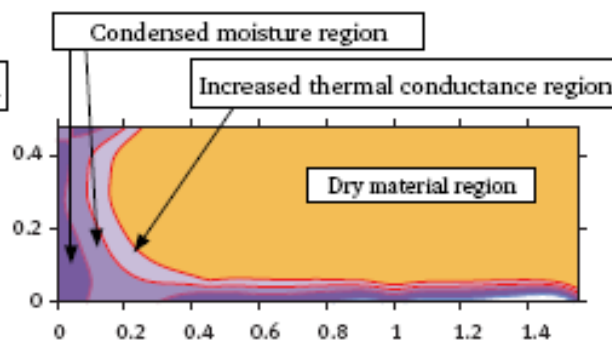


Fig. 6. Schematic presentation of moisture distribution in electrolysis cell foundation after 60-hour baking

The dewatered region of the cell foundation is adherent to the region of steam-water transformations. Depending on pore structure, material wetting in the considered region the pattern of heat and mass transfer can vary significantly. Circulating routes of moisture motion are formed. The resultant component of the mass transfer is directed from the center to the side walls with subsequent forcing of the moisture to the side walls of the cathode shell and increase of the «dry» region.

The same regions (dry, two-phase and overheated steam) after 60-hour baking are illustrated in Figure 2. The condensed moisture occupies the peripheral area near the side walls and narrow region near the bottom (including lower insulation layer). The lower boundary of the «dry» region in the middle portion of the foundation is located in the vicinity of the boundaries of thermal insulation layers 1 and 2.

At the end of baking (72 hours) there are only quantitative changes in the pattern. In the bottom region and in the lower thermal insulating layer there is condensed moisture, it results in temperature equalization in planar orientation. Thermal resistivity exists due to the upper (dry) layers of thermal insulation, the lower layer, impregnated with moisture, has higher thermal conductivity, this property is by an order higher in comparison with dry material.

Therefore, during baking process the thermal properties of cathode assembly foundation are determined mainly by moisture content. The moisture content, depending on electrolysis cell type, design of foundation and edge, state of materials, can vary in the range of from tens to hundreds kilograms.

The moisture occurrence results in more intensive heating of the foundation, however, the heat consumption for steam formation grows and the heat losses are increased (this value can be as high as 1000 MJ). In addition, as a result of steam formation, overpressure is created in the foundation and without draining channels it can be higher than 0.2 MPa resulting in disintegration of the lining.

With steam exhaust tubes after completion of baking of the cathode assembly residual moisture in the electrolysis cell foundation does not effect on the thermal state of lining and thermal insulation.

During operation the variations and uncertain thermal properties of the foundation are determined by the action of melts and vapors of fluorides on oxide lining and thermal insulation. At present the most typical design of the electrolysis cell cathode assembly includes carbon portion (bottom and side wall blocks and ramming paste), as well as oxide lining and thermal insulation (Figure 7).

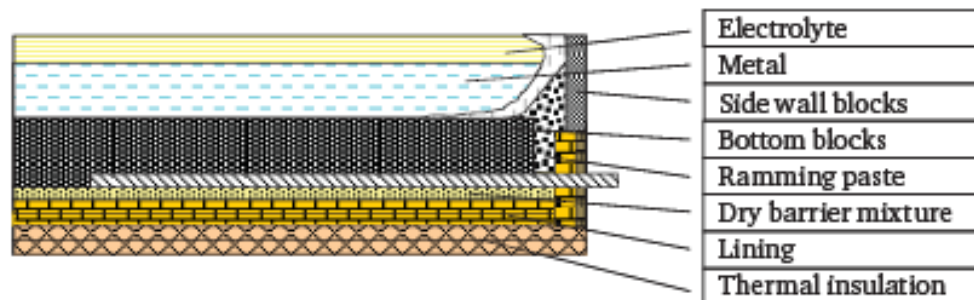


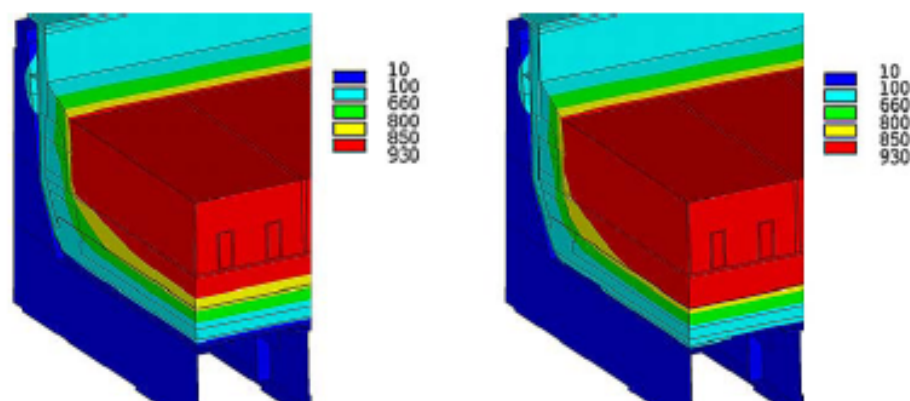
Fig. 7. Cathode schematic presentation

The purpose of the carbon bottom section consists of both cathode functions and formation of sealed reservoir for metal and electrolyte melts. However, taking into account actual factors (handling of cathode assemblies, heating thereof up to about 1000 °C, application of ramming pastes etc.) it is nearly impossible to provide the required sealing, only decrease of penetration of metal and fluorides can be provided. The rate of melt penetration under the bottom blocks is determined by the properties of the bottom blocks, ramming paste, performances of baking and start-up, design of foundation and edge, technological specifications, cell smelting geometry and some other factors. Penetrated melt interacts with the foundation materials, usually existing in form of alumina silicate refractory materials. At the same time thermal resistivity of the foundation in vertical direction is decreased.

Application of dry barrier mixtures, usually loose materials consisting of oxides ( $\text{SiO}_2$ ,  $\text{Al}_2\text{O}_3$ ,  $\text{CaO}$ ,  $\text{MgO}$ ,  $\text{Fe}_2\text{O}_3$ ), decreases but does not eliminate penetration of molten electrolyte. Application of pre-formed items as dry barrier materials allows to obtain higher density of the items decelerating the penetration rate but does not result in significant effect because joints and cracks create passages for the molten materials.

At overheating of the electrolysis cell foundation the solidus isotherm (881...888 °C) in the refractory materials and fluoride melt can reach the upper thermal insulating layers and this fact is crucial for cathode assembly.

Figure 8 illustrates estimated thermal state of an electrolysis cell at development stage in starting period of its operation and after partial impregnation of the foundation corresponding to 2–3 years of its operation with high-quality materials in its foundation.



$t_{\text{max}} = 66.9^\circ\text{C}$ ,  $Q_{\text{ext}} = 21.2 \text{ kW}$        $t_{\text{max}} = 93.5^\circ\text{C}$ ,  $Q_{\text{ext}} = 31.6 \text{ kW}$   
 a) – initial materials of the foundation      b) – impregnated materials of the foundation

Fig. 8. Comparison of cathode temperature fields with and without consideration of material impregnation with fluorides



In the course of operation lifetime of an electrolysis cell the temperature in the foundation grows, that is, the isotherms are «creeping down». This is especially characteristic for the top (refractory) portion of the foundation. However, the «ageing» of an electrolysis cell also occurs in the bottom portion. Excessive estimated temperature is increased by 26...27 °C (that is, 39...40 % relatively to the initial values), and the thermal losses across the bottom are increased by 10 kW (in fact, 1.5 fold).

The most efficient way to increase the lifetime of an electrolysis cell consists of a set of computational, engineering and organizational measures, including optimal choice of materials with consideration of overall set of technological parameters and thorough approach to arrangement of the foundation.

With the aim of obtaining of engineering estimations it is necessary to be aware of physical conditions of unambiguity in addition to other requirements. Wide set of physical properties should be considered because electrical and thermal problems are being solved simultaneously. The accuracy of the computational results depends mainly on electric conductivity of electrolyte and bottom block materials, thermal conductivity of carbon-graphite materials, refractory lining and thermal insulation. Moreover, it is necessary to consider for variations of properties of various materials resulting from the actions of fluorides.

The highest uncertainty at calculations of thermal state of cathode assembly results from thermal conductivity of refractory and thermal insulating materials in the course and in the end of the campaign.

Availability of wide scope of new materials and lining items in the market requires for investigations of temperature dependency of thermal conductivity at high temperatures and impregnation with fluorides at operation of electrolysis cells.

R&D Center «Power-Saving Technologies» developed and assembled the installation for estimation of thermal and electric conductivities of refractory and thermal insulating materials in the temperature range from ambient values to 1000 °C. Such installations allow to test materials with thermal conductivity of 0.1...5 W/(m K) and specific electric resistivity of from 20 μOhm·m to 0.001 Ohm·m

Schematic presentation of the installation for estimations of thermal conductivity is given in Figure 5.

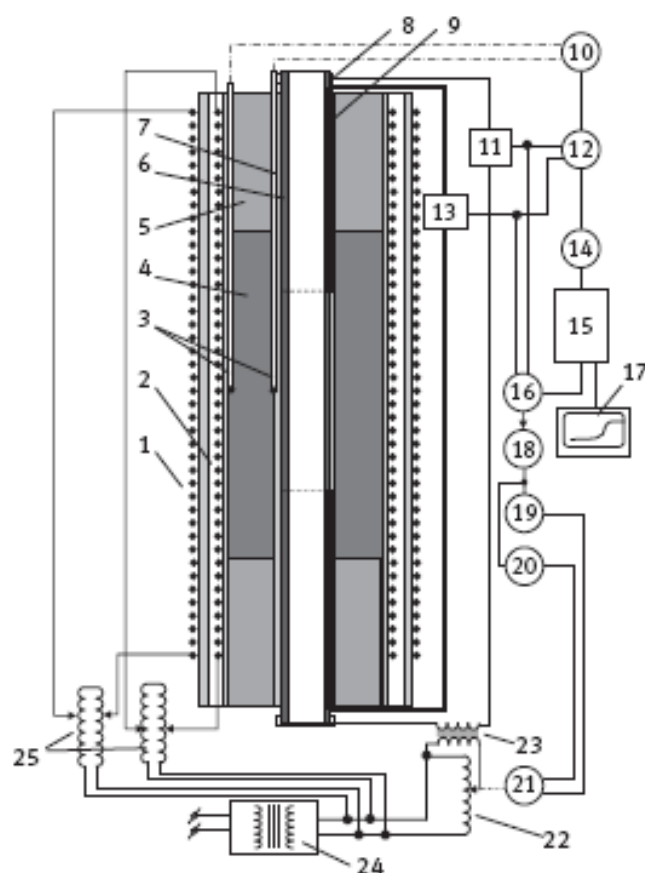


Fig. 5. Schematic presentation of experimental installation

The installation consists of 2 background electric heaters (Pos. 1, 2). The internal surface of the heater cylindrical casing serves as external surface of the measuring cell filled with tested material 4. The temperature drop at the tested material layer is measured by means the thermocouples 3. The tested material is restricted at the top and the bottom with the end plugs 5 made of thermal insulating materials. Along



the axis of the background heaters the main heater 6 is installed, assembled in the jacket 7. The voltage at the operating section of the main heater is determined by means of alternating current converter (Pos. 13) and the potential wires 9.

The thermocouples 3 are connected to the computer 15 via the 8-channel analog input module 10 and the interface converter 14, where their signals are processed and are displayed in real-time mode in the display 17.

The measurements of electric parameters are aided with one-channel alternating current normalizing transducers (Pos. 11) and alternating voltage converter (Pos. 13). The converters are connected to the 8-channel analog input module with galvanic decoupling (Pos. 12). The power of the main heater at the preset level is stabilized by means of equipment set consisting of industrial controller, normalizing converters 11 and 15, output and actuating devices, as well as power control elements. The power presets, regulating rules, estimation of the quality of the regulations are aided with the industrial computer 15.

## Conclusions

Optimization of energetic and economic performances of electrolysis cells at development stage is more efficient in combination with application of mathematical models.

Presently there are numerous available materials and products of various kinds and manufacturers. The data, obtained by R&D Center «Power-Saving Technologies», demonstrate that, for example, for ramming pastes from different suppliers, thermal conductivity can vary by a factor of 8, shrinkage – by a factor of 4, electric conductivity – by a factor of 2; for bottom blocks thermal conductivity can vary by a factor of 4 and higher, for lining materials – by a factor of 2, for thermal insulation – by a factor of 5.

There are no available data on physical properties of the utilized materials (initial and processed) in the operating temperature range. Therefore, wide scale investigations of the physical properties of the applied materials are highly required.

## REFERENCES

1. Teplovie protsessy v elektrolizerah i mikserah alyuminievogo proizvodstva: Monografiya / E. N. Panov, G.N. Vasil'chenko, S.V. Danilenko, A.Ya. Karvatskij, I.L. Shilovich, M.F. Bozhenko; Pod obsch. red. B.S. Gromova. – M.: Izdatel'skij dom «Ruda i metally», 1998. – 256 p. : ill., tabl. – Bibliogr. : p. 248–254.
2. Panov E. N. Sovremennije podhody k raschetu energeticheskogo balansa elektrolizera / E. N. Panov, A.Ya. Karvatskij, G.N. Vasil'chenko, I. L. Shilovich, V. V. Bil'ko // Alyuminij Sibiri – 2006 : XII Mezhdunar. konf., 5–7 sentyabrya 2006g. : Sb. dokladov. – Krasnoyarsk, 2006. – P. 97–101.
3. Karvatskij A.Ya. Primenenie chislennogo modelirovaniya dlya rascheta energobalansa alyuminievogo elektrolizera / A.Ya. Karvatskij, G.N. Vasil'chenko, V.V. Bil'ko // Promyshlennaya teplotehnika. – 2008. – T. 30, № 2. – P. 33–40.
4. Panov E.N. Physical processes modern investigation methods in power-intensive industrial equipments / E.N. Panov, A.Ya. Karvatsky, I.L. Shilovich, G.N. Vasilchenko, T.B. Shilovich, S.V. Leleka, S.V. Danilenko, V.V. Bilko, I.V. Pulinets, A.N. Chyzh // Aluminium of Siberia – 2008 : XIV International conference, 10–12 September 2008 : Proceedings. – Krasnoyarsk : «Verso», 2008. – P. 124–132.
5. Budilov I.N. Modelirovanie magnitno-gidrodinamicheskikh protsessov v promyshlennykh elektrolizerah s pomosh'yu ANSYS / Budilov I.N., Lukaschuk Yu.V. // ANSYS Solutions. Russkaya redaktsia. – Osen' 2007. – P. 13–18.
6. Patankar S. Chislennye metody resheniya zadach teploobmena i dinamiki zhidkosti / Segerlind L. ; per. s angl. V.D. Vilenskogo. – M.: Energoatomizdat, 1984. – 153 p. : ill., tabl. – Bibliogr. : p. 145–148.
7. Spravochnik metallurga po tsvetnym metallam. Proizvodstvo alyuminiya / Pod red. Yu.V. Baimakova, Ya.E. Kontorovicha. – M.: Metallurgiya, 1971. – 560 p.
8. Kiss, L.I., Poncsak S.: Effect of the bubble growth mechanism on the spectrum of voltage fluctuations in the reduction cell, TMS Light Metals, pp. 139–145, 2002.
9. Perron A, Kiss L, Poncsak S.: Regimes of the movement of bubbles under the anode in an aluminum electrolysis cell. TMS, Light Metals, 2005.
10. Teploperedacha v dvuhfaznom potoke / Pod red. D.Battervorsa i G.Hyuitta: Per. s angl. – M.: Energiya, 1980. – 328 p.;
11. Kutateladze S.S. Teploperedacha i gidrodinamicheskoe soprotivlenie. Spravochnoe posobie. – M.: Energoatomizdat, 1990. – 367 p.
12. Yanko E.A. Anody alyuminievykh elektrolizerov. – M.: Izdatel'skij dom «Ruda i metally», 2001. – 670 p.